MATHEMATICAL MODELING AND COMPUTING, Vol. 9, No. 4, pp. 816–824 (2022)

Double solutions and stability analysis of slip flow past a stretching/shrinking sheet in a carbon nanotube

Norzawary N. H. A.[1], Bachok N.[1,2], Ali F. M.[1,2], Rahmin N. A. A.[2]

[1] *Institute for Mathematical Research, Universiti Putra Malaysia, 43400 Serdang, Selangor, Malaysia*
[2] *Department of Mathematics and Statistics, Faculty of Science, Universiti Putra Malaysia, 43400 Serdang, Selangor, Malaysia*

(Received 11 August 2022; Accepted 3 September 2022)

A stagnation point flow past a stretching/shrinking surface in carbon nanotubes (CNTs) with slip effects is investigated in this paper. Applying transformations of similarity, the governing partial differential equations are modified to the nonlinear ordinary differential equations. Afterward, they are numerically solved in Matlab by the bvp4c solver. The single-wall CNTs and multi-wall CNTs are used, including water as a base fluid. The effects of the flow parameters are investigated, shown in the form of graphs, and physically evaluated for the dimensionless velocity, temperature, skin friction, and Nusselt numbers. According to our findings, the unique solution exists for stretching sheets, whereas non-unique solutions are obtainable for shrinking sheets. The stability analysis is utilized to discover which solution is stable.

Keywords: *carbon nanotube, dual solutions, stagnation point flow, stretching/shrinking sheet, slip effects, stability analysis.*

2010 MSC: 76D10, 35Q79, 80A20, 76A02, 35Q35 **DOI:** 10.23939/mmc2022.04.816

1. Introduction

A fluid flow on a solid surface's stagnation area is known as a stagnation point flow where fluid approaching the surface divides into different streams. Hiemenz [1] is the first person who studied the two-dimensional (2D) stagnation point flow through the static semi-infinite wall, where he reduced the Navier–Stokes equations to the nonlinear ordinary differential equations by means of similarity transformations. After that, Homann [2] extended problem [1] by considering axisymmetric stagnation point flow. Solution for stagnation point flows and stretching sheet were examined by Mahapatra and Gupta [3, 4]. Crane [5] analyzed the 2D boundary layer flow brought on elastic plain stretching sheet while moving in its plane. However, Khan and Pop [6] are the first who investigated the problem on stretching sheet in nanofluids. Following the publication of this seminal study, other researchers have looked into the research problem of the fluid flow field of a stagnation point toward a stretch/shrink surface [7–9].

Nowadays, there are many studies on nanofluids due to industrial application demand. One of the reason is, nanofluid's behavior is giving a big impact on enhancing heat transfer in applications such as transportation, electronics and biomedicine. Choi [10] is the first person who introduced nanofluid which consists of nanometer-sized particles known as nanoparticles. Although there are several materials that could be employed to create nanoparticles, carbon exhibits good outcomes resulting from its strong electrical, mechanical, and thermal characteristics. Hence, Choi et al. [11] explored the thermal capability of oil-based CNT. CNTs are a type of carbon allotrope that is a tube-shaped structure with a diameter that is measured in nanometers and comprise of single wall (SWCNTs) and multi wall (MWCNTs).

In comparison to other nanoparticles with a similar volume fraction, suspensions of carbon nanotubes have better thermal characteristics [12, 13]. In this manner, carbon nanotubes can enhance the thermal conductivity of base fluids as well as convective heat transfer. Ever since, numerous studies have discovered the CNTs' benefits and examined numerous boundary layer issues on CNTs [14–16].

Researchers in earlier studies just examined the flow field that just complies with the no-slip boundary condition, which then make it necessary to study the effect of slip boundary conditions. Bhattacharyya et al. [17, 18] explored the boundary layer slip flow via flat plate and also on a moving plate. The heat transfer and fluid flow of CNTs towards a flat plate under Navier slip boundary conditions were initially studied by Khan et al. [19]. After that, several papers also took slip effects into account [20–22].

The goal of this paper is to continue on the research conducted by Bachok et al. [23]. While they were considering stagnation point flow in a nanofluid, this paper consider stagnation point flow for both single-walled and multi-walled CNTs with water base fluid.

2. Methodology

Consider a 2D, steady and incompressible flow within scope $y > 0$ guided by a stretch/shrink sheet at $y = 0$ with a fixed point of stagnation $x = 0$. Since a and b are constants with $b > 0$, it is assumed that the stretch/shrink velocity $U_w(x) = ax$ and the ambient fluid velocity $U_\infty(x) = bx$ both vary linearly from the point of stagnation. The following is a possible formulation for the boundary layer equations [23]:

$$\frac{\partial u}{\partial x} + \frac{\partial v}{\partial y} = 0, \tag{1}$$

$$u\frac{\partial u}{\partial x} + v\frac{\partial u}{\partial y} = U_\infty \frac{dU_\infty}{dx} + \frac{\mu_{nf}}{\rho_{nf}}\frac{\partial^2 u}{\partial y^2}, \tag{2}$$

$$u\frac{\partial T}{\partial x} + v\frac{\partial T}{\partial y} = \alpha_{nf}\frac{\partial^2 T}{\partial y^2} \tag{3}$$

and the boundary conditions are

$$\begin{gathered} v = 0, \quad u = U_w + L\frac{\partial u}{\partial y}, \quad T = T_w \quad \text{at} \quad y = 0, \\ u \to U_\infty, \quad T \to T_\infty, \quad \text{as} \quad y \to \infty. \end{gathered} \tag{4}$$

The velocity components in directions of x and y are respectively u and v, nanofluid's temperature is T, and length of slip is L. α_{nf}, ρ_{nf} and μ_{nf} are the thermal diffusivity, density and viscosity of the nanofluid, accordingly, that are provided by Oztop and Abu–Nada [24]:

$$\alpha_{nf} = \frac{k_{nf}}{(\rho C_p)_{nf}}, \quad \rho_{nf} = (1-\varphi)\rho_f + \varphi\rho_{CNT}, \quad \mu_{nf} = \frac{\mu_f}{(1-\varphi)^{2.5}},$$

$$(\rho C_p)_{nf} = (1-\varphi)(\rho C_p)_f + \varphi(\rho C_p)_{CNT}, \quad \frac{k_{nf}}{k_f} = \frac{1-\phi+2\phi\frac{k_{CNT}}{k_{CNT}-k_f}\ln\frac{k_{CNT}+k_f}{2k_f}}{1-\phi+2\phi\frac{k_f}{k_{CNT}-k_f}\ln\frac{k_{CNT}+k_f}{2k_f}},$$

where CNTs volume fraction is φ, $(\rho C_p)_{nf}$, k_{nf} are the heat capacity and thermal conductivity of nanofluid, while k_{CNT}, $(\rho C_p)_{CNT}$, ρ_{CNT} are the thermal conductivity, heat capacity and densities of CNTs, sequentially, and k_f for fluid's densities. The term $\frac{k_{nf}}{k_f}$ was adapted from Xue [25] in which the Maxwell theory model consider the impacts of CNTs space distribution on heat conductivity.

By adopting the following transformation, the governing Eqs. (1)–(3) and conditions (2) can be expressed more simply as

$$\psi = (bv_f)^{\frac{1}{2}} x f(\eta), \quad \eta = \left(\frac{b}{v_f}\right)^{\frac{1}{2}} y, \quad \theta(\eta) = \frac{T - T_\infty}{T_w - T_\infty}, \tag{5}$$

where the variable of similarity is η and function of stream is ψ described as $u = \frac{\partial\psi}{\partial y}$ and $v = -\frac{\partial\psi}{\partial x}$, that comply with Eq. (1) equivalently. Eqs. (2)–(3) and conditions (2) can be simplified to the following ODEs by using Eq. (5):

$$Af''' + ff'' - f'^2 + 1 = 0, \tag{6}$$

$$\frac{B}{\Pr}\theta'' + f\theta' = 0, \tag{7}$$

$$f(0) = 0, \quad f'(0) = \varepsilon + \sigma f''(0), \quad \theta(0) = 1,$$
$$f'(\eta) \to 1, \quad \theta(\eta) \to 0, \quad \text{as} \quad \eta \to \infty, \tag{8}$$

where $A = \frac{1}{(1-\varphi)^{2.5}(1-\varphi+\varphi\rho_{CNT}/\rho_f)}$, $B = \frac{k_{nf}/k_f}{1-\varphi+\varphi(\rho C_p)_{CNT}/(\rho C_p)_f}$, $\sigma = L\left(\frac{b}{v_f}\right)^{\frac{1}{2}}$ is the parameter of slip and $\varepsilon = \frac{a}{b}$ is the parameter of velocity ratio which for stretching is when $\varepsilon > 0$ and shrinking is when $\varepsilon < 0$.

The number of local Nusselt Nu_x and the coefficient of skin friction C_f are the physical quantities of concern in this study,

$$C_f = \frac{\mu_{nf}}{\rho_f U_\infty^2}\left(\frac{\partial u}{\partial y}\right)_{y=0}, \quad \mathrm{Nu}_x = -\frac{x k_{nf}}{k_f(T_w - T_\infty)}\left(\frac{\partial T}{\partial y}\right)_{y=0}$$

The quantities of physical interest that we acquire following transformations are

$$C_f \,\mathrm{Re}_x^{1/2} = (1-\varphi)^{-2.5} f''(0), \quad \mathrm{Nu}_x \,\mathrm{Re}_x^{-1/2} = -\frac{k_{nf}}{k_f}\theta'(0) \tag{9}$$

where $\mathrm{Re}_x = \frac{U_\infty x}{\nu_f}$ is the number of Reynolds.

Stability analysis is carried out to identify the smallest unknown eigenvalue. That is because the results give the same interpretation, where the first solution is stable, whereas the second solution is non stable and this finding was corroborated by many researchers [26–28]. The unsteady case is introduced to perturb the Eqs. (2)–(3) which is replaceable with

$$\frac{\partial u}{\partial t} + u\frac{\partial u}{\partial x} + v\frac{\partial u}{\partial y} = U_\infty \frac{dU_\infty}{dx} + \frac{\mu_{nf}}{\rho_{nf}}\frac{\partial^2 u}{\partial y^2}, \tag{10}$$

$$\frac{\partial T}{\partial t} + u\frac{\partial T}{\partial x} + v\frac{\partial T}{\partial y} = \alpha_{nf}\frac{\partial^2 T}{\partial y^2}. \tag{11}$$

The new similarity transformation is introduced as follows

$$\psi = (v_f b)^{\frac{1}{2}} x f(\eta, \tau), \quad \eta = \left(\frac{b}{v_f}\right)^{\frac{1}{2}} y, \quad \theta(\eta, \tau) = \frac{T - T_\infty}{T_w - T_\infty}, \quad \tau = bt. \tag{12}$$

Implementing the new transformation given in Eq. (12) into Eqs. (10)–(11), we obtain:

$$A\frac{\partial^2 \theta}{\partial \eta^2} + f\frac{\partial \theta}{\partial \eta} - \frac{\partial \theta}{\partial \tau} = 0, \tag{13}$$

$$\frac{B}{\Pr}\frac{\partial^2 \theta}{\partial \eta^2} + f\frac{\partial \theta}{\partial \eta} - \frac{\partial \theta}{\partial \tau} = 0. \tag{14}$$

Subject to the boundary conditions

$$f(0,\tau) = 0, \quad \frac{\partial f}{\partial \eta}(0,\tau) = \varepsilon + \sigma\frac{\partial^2 f}{\partial \eta^2}(0,\tau), \quad \theta(0,\tau) = 1,$$
$$\frac{\partial f}{\partial \eta}(\eta,\tau) \to 1, \quad \theta(\eta,\tau) \to 0 \quad \text{as} \quad \eta \to \infty.$$

Next, the following equations are used to detect the stability of the flow [29]:

$$f(\eta,\tau) = f_0(\eta) + e^{-\gamma\tau}F(\eta,\tau), \quad \theta(\eta,\tau) = \theta_0(\eta) + e^{-\gamma\tau}G(\eta,\tau), \tag{15}$$

where γ is parameter of unknown eigenvalue, $F(\eta)$ and $G(\eta)$ are small relative to $f_0(\eta)$ and $\theta_0(\eta)$, respectively. Using Eq. (15) into (13)–(14) and letting $\tau \to 0$, where $F(\eta) = F_0(\eta)$ and $G(\eta) = G_0(\eta)$, we have the linearized equation as follows:

$$AF_0''' + f_0F_0'' - (2f_0' - \gamma)F' = 0,$$
$$\frac{B}{\Pr}G_0'' + f_0G_0' + F\theta_0' + \gamma G_0 = 0,$$

$$F_0'(0) = \sigma F_0''(0), \quad F_0(0) = 0, \quad G_0(0) = 0,$$
$$F_0'(\eta) \to 0, \quad G_0(\eta) \to 0.$$

Following the work of Harris et al. [30], one of the boundary conditions need to be relaxed. Hence, we changed $F_0'(\eta) \to 0$ as $\eta \to \infty$ with the new condition $F_0''(\eta) = 1$.

3. Results and discussion

The bvp4c solver in Matlab is used to numerically solve the system of Eqs. (6)–(7) and the conditions in (8). With water as the base fluid, we take into consideration both SWCNTs and MWCNTs. Citing Oztop and Abu–Nada [24] as sources, the range of the volume fraction of CNTs that we have taken into consideration is $0 \leqslant \varphi \leqslant 0.2$, where $\varphi = 0$ is a regular fluid with a Prandtl number of $\mathrm{Pr} = 6.2$. Table 1 is a list of the CNTs' and the base fluid's thermophysical characteristics.

Table 1. Thermophysical properties of CNTs (Khan et al. [19]).

Physical properties	Base fluid	Nanoparticles SWCNTs	MWCNTs
ρ (kg/m^3)	997	2600	1600
c_p (J/kg K)	4179	425	796
k (W/m K)	0.613	6600	3000

The variation and comparison of $f''(0)$ with earlier research that is documented in the literature, which is Bachok et al. [23], are shown in Table 2, which demonstrates a positive accordance and so provides assurance that the numerical results produced are valid. In addition, Table 2 also contains the $f''(0)$ values for $\varphi \neq 0$ for future references.

Table 2. $f''(0)$ values for some ε and φ with water base fluid.

ε	Bachok et al. [23]	Present results		
	$\varphi = 0$	$\varphi = 0$	$\varphi = 0.1$	$\varphi = 0.2$
2	−1.88731	−1.88731	−1.78244	−1.64150
1	0	0	0	0
0.5	0.71330	0.71330	0.67366	0.62039
0	1.23259	1.23259	1.16410	1.07205
−0.5	1.49567	1.49567	1.41527	1.30087
−1	1.32882	1.32882	1.25499	1.15575
	[0]	[0]	[0]	[0]
−1.15	1.08223	1.08223	1.02210	0.94128
	[0.11670]	[0.11670]	[0.11022]	[0.10150]
−1.2	0.93247	0.93247	0.88066	0.81103
	[0.23365]	[0.23365]	[0.22067]	[0.20322]
−1.2465	0.58428	0.58428	0.55182	0.50818
	[0.55430]	[0.55430]	[0.52350]	[0.48210]

[ ] Second solution

Figure 1 displays the variety of $f''(0)$ and $-\theta'(0)$ with several values of the stretching/shrinking parameter ε, for three different values of CNTs volume fraction φ, where $\varphi = 0$, 0.1 and 0.2 for water-SWCNTs when $\mathrm{Pr} = 6.2$. There are dual solutions, as can be observed when $\varepsilon_c < \varepsilon \leqslant -1$, also there is a unique solution exists when $\varepsilon > -1$ and no solutions for $\varepsilon < \varepsilon_c < 0$ (ε_c — critical value of ε). These figures allow us to deduce that an increment of φ improves skin friction while decreasing surface's heat transfer.

Figure 2 show the divergence of $f''(0)$ and $-\theta'(0)$ with several values of ε, for three different values of slip parameter σ, where $\sigma = 0$, 0.2 and 0.4 for water base fluid when $\mathrm{Pr} = 6.2$ and $\varphi = 0.1$. The range of ε values where a solution exists expands as σ grows ($\varepsilon \geqslant \varepsilon_c$). The value of $\varepsilon_c = -1.2465$ for $\varphi = 0.1$ and $\sigma = 0$ shows a good agreement with Bachok et al. [23].

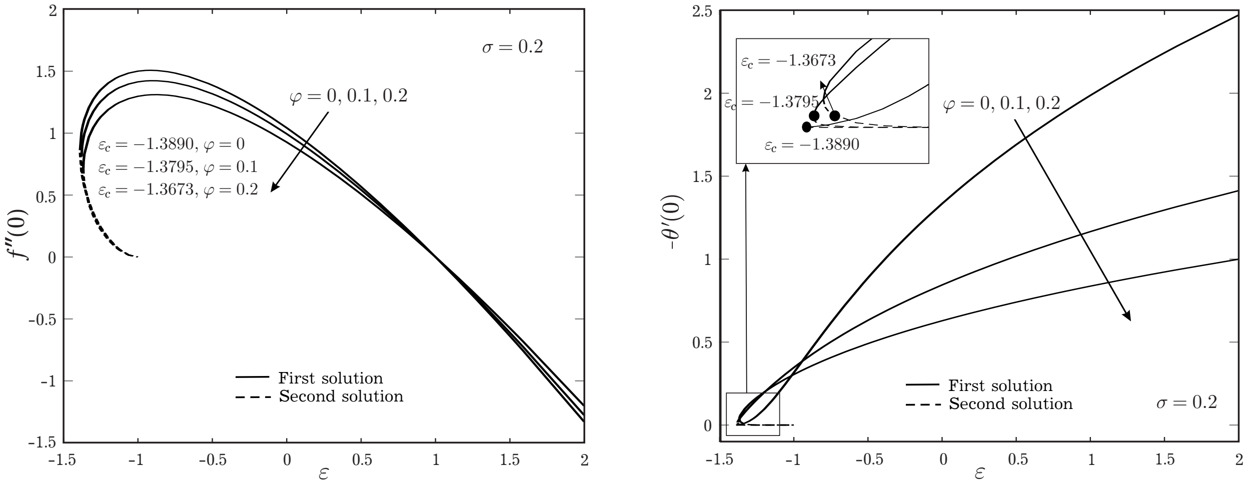

a ***b***

Fig. 1. (***a***) $f''(0)$ and (***b***) $-\theta'(0)$ graphs for φ and ε with water-SWCNT, respectively.

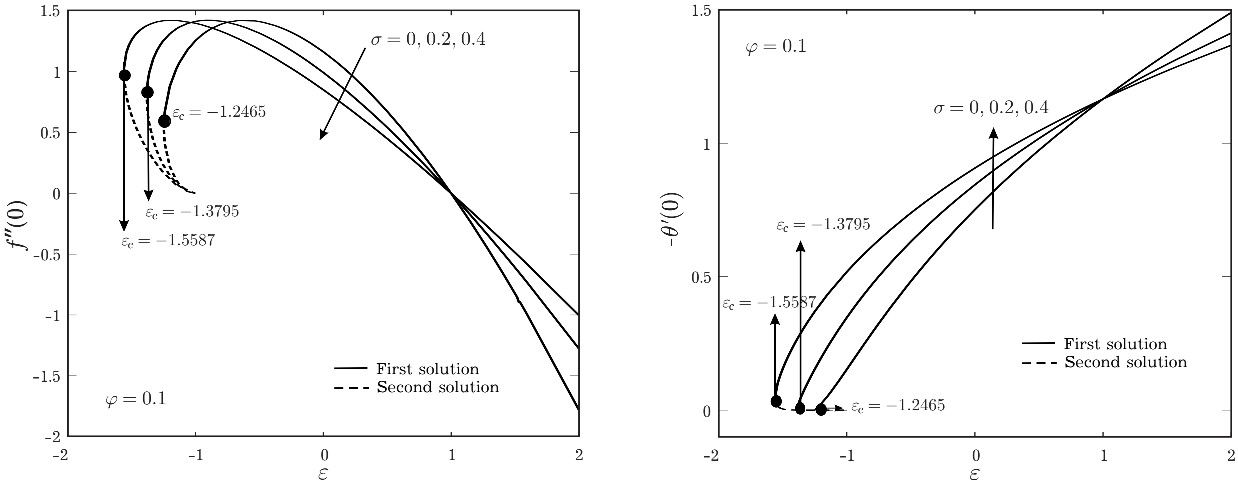

a ***b***

Fig. 2. (***a***) $f''(0)$ and (***b***) $-\theta'(0)$ graphs for σ and ε with water-SWCNT, respectively.

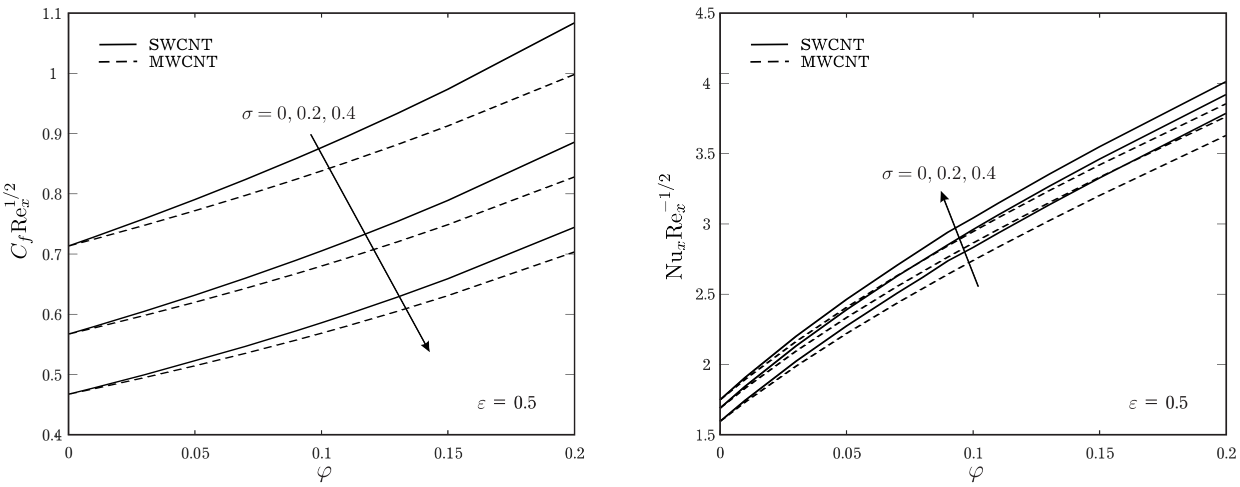

a ***b***

Fig. 3. (***a***) $C_f \mathrm{Re}_x^{1/2}$ and (***b***) $\mathrm{Nu}_x\, \mathrm{Re}_x^{-1/2}$ with φ for different σ.

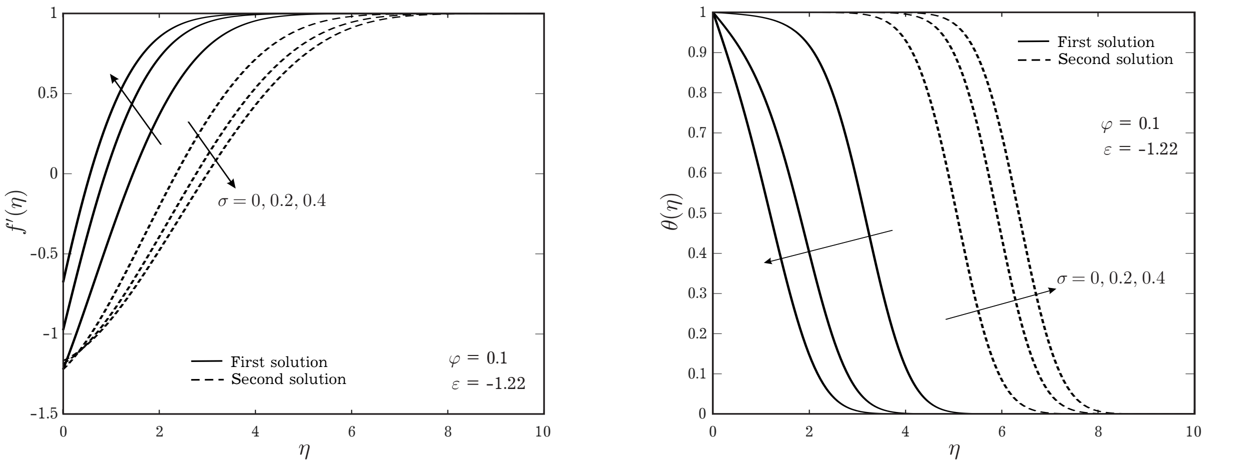

a ***b***

Fig. 4. (***a***) Velocity and (***b***) temperature profiles for σ and water-MWCNTs, respectively.

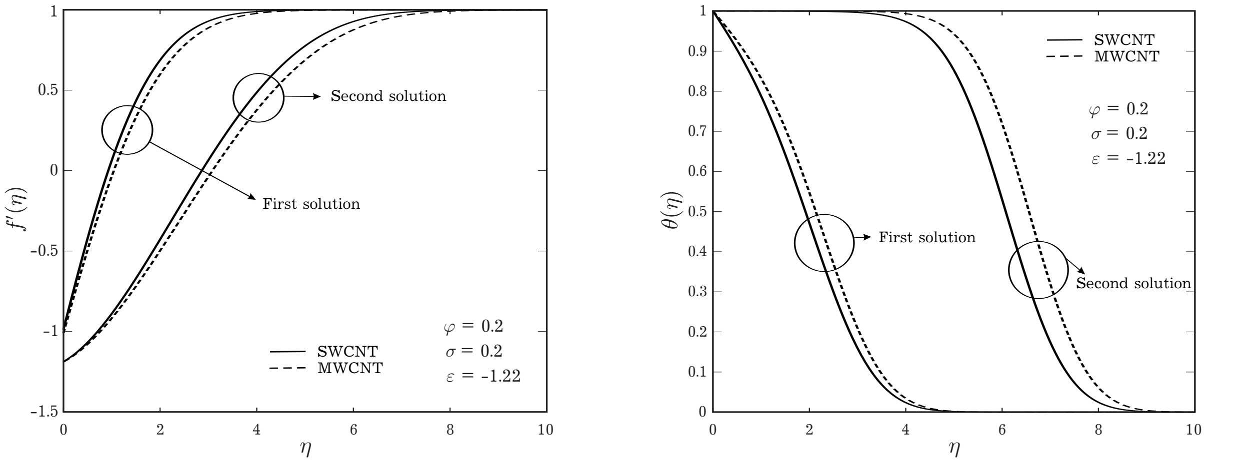

a ***b***

Fig. 5. (***a***) Velocity and (***b***) temperature profiles for various carbon nanotubes for water base fluid, respectively.

$C_f \operatorname{Re}_x^{1/2}$ and $\operatorname{Nu}_x \operatorname{Re}_x^{-1/2}$, given by Eq. (9) are illustrated in Figure 3 with φ for three different values of slip parameter which are $\sigma = 0$, 0.2 and 0.4, with $\varepsilon = 0.5$. It is inferred that $C_f \operatorname{Re}_x^{1/2}$ reduces as the slip parameter increases, whereas $\operatorname{Nu}_x \operatorname{Re}_x^{-1/2}$ rises which conclude that slip presence enhance the surface's heat transfer. It is also discovered that SWCNTs have higher $C_f \operatorname{Re}_x^{1/2}$ and $\operatorname{Nu}_x \operatorname{Re}_x^{-1/2}$ than MWCNTs due to their higher density and thermal conductivity, refer to Table 1.

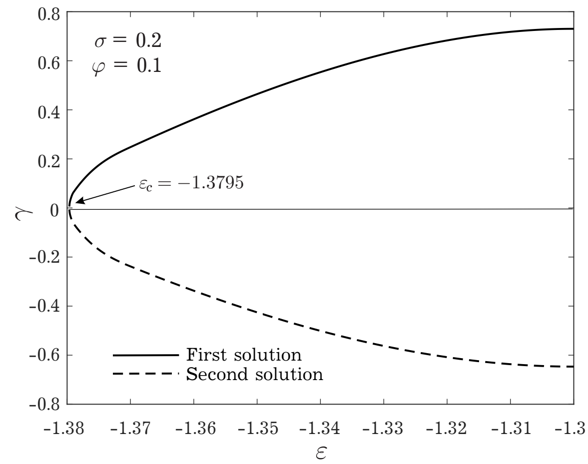

Fig. 6. γ at selected ε for $\sigma = 0.2$ and $\varphi = 0.1$ for water–SWCNTs.

Figures 4–5 display the profiles of velocity and temperature for a selection of parameter values. Both the first and second solutions are referred to in terms of the curves in Figures 1–2, with the first solution having greater values for $f''(0)$ and $-\theta'(0)$ than the second solution. These profiles asymptotically satisfy the conditions (8) indicating the existence of the dual solutions depicted in Figures 1–2.

Figure 4 presents the profiles for velocity and temperature for different value of slip parameter, where $\sigma = 0$, 0.2 and 0.4 when $\varphi = 0.1$ and $\varepsilon = -1.22$. The velocity profile is observed to increase in the first solution and drop in the second solution as σ

increases, while the temperature profile declines. While, Figure 5 presents the profiles for velocity and temperature for different types of CNTs which are SWCNT and MWCNT, with $\sigma = 0.2$, $\varphi = 0.2$, $\varepsilon = -1.22$ and water base fluid where SWCNT is discovered to have a higher temperature and velocity than MWCNT.

Figure 6 presents the smallest eigenvalues γ for different values of ε. For the upper branch solution, the smallest own values are shown to be positive, while the opposite is true for the lower branch solution. Figure 6 also shows how γ approaches 0 for both similarity solutions as $\varepsilon \to \varepsilon_c$, which supports the idea that γ is equal to zero when $\varepsilon = \varepsilon_c$. Because of this, the first solution was more stable than the second.

4. Conclusion

The impacts of CNTs volume fraction and effect of slip on the stagnation point flow past a stretching/shrinking sheet were examined theoretically and analysed in this study. The problem was resolved using the Matlab bvp4c solver. The findings show that

1. Unique solutions exist for stretching sheets, while dual solutions exist for shrinking sheets.
2. With an increase in slip, the range of solutions expands.
3. Skin friction declines as the slip parameter rises, while heat transmission increases.
4. For both: skin friction and the number of local Nusselt, single-walled CNTs are more effective than multi-walled CNTs.
5. According to the stability study, the first solution is stable and the second solution is not stable.

[1] Hiemenz K. Die Grenzchicht an einem in den gleichfromigen Flussigkeitsstrom eingetauchten geraden Kreiszylinder. Dingler's Polytech J. **326**, 321–324 (1911).

[2] Homann F. Der Einfluß grosser Zähigkeit bei der Strömung um den Zylinder und um die Kugel. Zeutschrift für Angewandte Mathematik und Mechanik. **16**, 153–164 (1936).

[3] Mahapatra T. R., Gupta A. S. Heat transfer in stagnation-point flow towards a stretching sheet. Heat Mass Transfer. **38**, 517–521 (2002).

[4] Mahapatra T. R., Gupta A. S. Stagnation-point flow towards a stretching surface. The Canadian Journal of Chemical Engineering. **81** (2), 258–263 (2003).

[5] Crane L. J. Flow Past a Stretching Plate. Zeitschrift für angewandte Mathematik und Physik. **21**, 645–647 (1970).

[6] Khan A. V., Pop I. Boundary-layer flow of a nanofluid past a stretching sheet. International Journal of Heat and Mass Transfer. **53** (11–12), 2477–2483 (2010).

[7] Nadeem S., Khan M. R., Khan A. U. MHD oblique stagnation point flow of nanofluid over an oscillatory stretching/shrinking sheet: existence of dual solutions. Physica Scripta. **94** (7), 075204 (2019).

[8] Nadeem S., Rehman M. I., Saleem S., Bonyah E. Dual solutions in MHD stagnation point flow of nanofluid induced by porous stretching/shrinking sheet with anisotropic slip. AIP Advances. **10** (6), 065207 (2020).

[9] Zainal N. A., Nazar R., Naganthran K., Pop I. Unsteady Stagnation Point Flow of Hybrid Nanofluid Past a Convectively Heated Stretching/Shrinking Sheet with Velocity Slip. Mathematics. **8** (10), 1649 (2020).

[10] Choi S. U. S., Eastman J. A. Enhancing thermal conductivity of fluids with nanoparticles. ASME Publ.-Fed. **231**, 99–106 (1995).

[11] Choi S. U. S., Zhang Z. G., Yu W., Lockwood F. E., Grulke E. A. Anomalous thermal conductivity enhancement in nanotube suspensions. Applied Physics Letters. **79** (14), 2252–2254 (2001).

[12] Mare T., Halelfadl S., Sow O., Estelle P., Duret S., Bazantay F. Comparison of the thermal performances of two nanofluids at low temperature in a plate heat exchanger. Experimental Thermal and Fluid Science. **35** (8), 1535–1543 (2011).

[13] Liu M. S., Lin M. C. C., Huang I. T., Wang C. C. Enhancement of thermal conductivity with carbon nanotube for nanofluids. International Communications in Heat and Mass Transfer. **32** (9), 1202–1210 (2005).

[14] Sreedevi P., Reddy P. S., Chamka A. J. Magneto-hydrodynamics heat and mass transfer analysis of single and multi-wall carbon nanotubes over vertical cone with convective boundary condition. International Journal of Mechanical Sciences. **135**, 646–655 (2018).

[15] Norzawary N. H. A., Bachok N., Ali F. M. Stagnation Point Flow over a Stretching/Shrinking Sheet in a Carbon Nanotubes with Suction/Injection Effects. CFD Letters. **20** (2), 106–114 (2020).

[16] Othman M. N., Jedi A., Bakar N. A. A. MHD Stagnation Point on Nanofluid Flow and Heat Transfer of Carbon Nanotube over a Shrinking Surface with Heat Sink Effect. Molecules. **26** (24), 7441 (2021).

[17] Bhattacharyya K., Mukhopadhyay S., Layek G. C. Steady boundary layer slip flow and heat transfer over a flat porous plate embedded in a porous media. Journal of Petroleum Science and Engineering. **78** (2), 304–309 (2011).

[18] Bhattacharyya K., Layek G. C., Gorla R. S. R. Slip effect on boundary layer flow on a moving flat plate in a parallel free stream. International Journal of Fluid Mechanics Research. **39** (5), 438–447 (2012).

[19] Khan W. A., Khan Z. H., Rahi M. Fluid flow and heat transfer of carbon nanotubes along a flat plate with Navier slip boundary. Applied Nanoscience. **4**, 633–641 (2014).

[20] Bachok N., Najib N., Ariffin N. M., Senu N. Stability of dual solutions in boundary layer flow and heat transfer on a moving plate in a copper-water nanofluid with slip effect. WSEAS Transactions on Fluid Mechanics. **11**, 151–158 (2016).

[21] Najib N., Bachok N., Ariffin N. M., Senu N. Boundary layer flow and heat transfer of nanofluids over a moving plate with partial slip and thermal convective boundary condition:stability analysis. International Journal of Mechanic. **11**, 18–24 (2016).

[22] Anuar N. S., Bachok N., Pop I. A stability analysis of solutions in boundary layer flow and heat transfer of carbon nanotubes over a moving plate with slip effect. Energies. **11** (12), 3243 (2018).

[23] Bachok N., Ishak A., Pop I. Stagnation-point flow over a stretching/shrinking sheet in a nanofluid. Nanoscale Research Letters. **6**, 623 (2011).

[24] Oztop H. F., Abu–Nada E. Numerical study of natural convection in partially heated rectangular enclosures filled with nanofluids. International Journal of Heat and Fluid Flow. **29** (5), 1326–1336 (2008).

[25] Xue Q. Z. Model of thermal conductivity of carbon nanotube-based composites. Physica B: Condensed Matter. **368** (1–4), 302–307 (2005).

[26] Anuar N. S., Bachok N., Arifin N. M., Rosali H. MHD flow past a nonlinear stretching/shrinking sheet in carbon nanotubes: Stability analysis. Chinese Journal of Physics. **65**, 436–446 (2020).

[27] Anuar N. S., Bachok N., Turkyilmazoglu M., Arifin N. M., Rosali H. Analytical and stability analysis of MHD flow past a nonlinearly deforming vertical surface in Carbon Nanotubes. Alexandria Engineering Journal. **59** (1), 497–507 (2020).

[28] Banerjee A., Bhattacharyya K., Mahato S. K., Chamka A. J. Influence of various shapes of nanoparticles on unsteady stagnation-point flow of Cu-H_2O nanofluid on a flat surface in a porous medium: A stability analysis. Chinese Physics B. **31** (4), 044701 (2022).

[29] Weidman P. D., Kubitschek D. G., Davis A. M. J. The effect of transpiration on self-similiar boundary layer flow over moving surfaces. International Journal of Engineering Science. **44** (11–12), 730–737 (2006).

[30] Harris S. D., Ingham D. B., Pop I. Mixed convection boundary-layer flow near the stagnation point on a vertical surface in a porous medium: Brinkman model with slip. Transport in Porous Media. **77**, 267–285 (2009).

Подвійні розв'язки та аналіз стійкості ковзаючого обтікання листа, що розтягується/стискається, у вуглецевих нанотрубках

Норзавари Н. Х. А., Бачок Н., Алі Ф. М., Рахмін Н. А. А.

[1] *Інститут математичних досліджень,*
Університет Путра Малайзії,
43400 Серданг, Селангор, Малайзія
[2] *Кафедра математики та статистики,*
Факультет природничих наук,
Університет Путра Малайзія,
43400 Серданг, Селангор, Малайзія

У цій статті досліджується потік через точку застою поверхні, що розтягується/стискається, у вуглецевих нанотрубках (ВНТ) з ефектами ковзання. Застосовуючи перетворення подібності, основні диференціальні рівняння в частинних похідних модифікуються, щоб отримати нелінійні звичайні диференціальні рівняння. Потім вони чисельно розв'язуються в Matlab за допомогою розв'язувача bvp4c. Застосовуються одностінні та багатостінні ВНТ; вода слугує базовою рідиною. Досліджено вплив параметрів потоку, який продемонстровано у вигляді графіків і фізично оцінено для таких величин: безрозмірна швидкість, температура, поверхневе тертя та числа Нуссельта. Згідно з отриманими даними, однозначні розв'язки існують для листів, що розтягуються, тоді як для листів, що стискаються, отримано неоднозначні розв'язки. Аналіз стійкості застосовується, щоб визначити, який розв'язок є стійким.

Ключові слова: *вуглецеві нанотрубки, подвійні розв'язки, потік точки застою, розтягування/стискання листа, ефекти ковзання, аналіз стійкості.*